

Anisotropic seismic structure of the lithosphere beneath the Adriatic coast of Italy constrained with mode-converted body waves

Vadim Levin,¹ Lucia Margheriti,² Jeffrey Park,¹ and Alessandro Amato²

Received 7 May 2002; revised 26 August 2002; accepted 3 September 2002; published 26 November 2002.

[1] P_S converted waves observed near Ancona on the Adriatic coast of central Italy, as revealed by teleseismic receiver functions (RFs), vary with earthquake back-azimuth and epicentral distance in a manner consistent with a 1-D anisotropic seismic structure. Using reflectivity calculations, we develop a profile of anisotropic seismic velocity through the Adriatic lithosphere at this locality. We infer crustal thickness of ~ 45 km. Anisotropy within the crust appears at ~ 15 -km depth, suggesting a decollement between the subducting Adriatic lithosphere and the overriding crustal wedge. Lineation of inferred rock fabric is compatible with simple shear in ENE-WSW direction. In the upper mantle, we infer an anisotropic layer at 80–90 km depth. If caused by olivine crystals alignment, the nearly north-south lineation of the inferred rock fabric would be consistent with some nearby shear-wave splitting observations. This anisotropic layer may be related to mantle deformation induced by the rollback of Adriatic lithosphere. **INDEX TERMS:** 7203 Seismology: Body wave propagation; 7218 Seismology: Lithosphere and upper mantle; 8102 Tectonophysics: Continental contractional orogenic belts. **Citation:** Levin, V., L. Margheriti, J. Park, and A. Amato, Anisotropic seismic structure of the lithosphere beneath the Adriatic coast of Italy constrained with mode-converted body waves, *Geophys. Res. Lett.*, 29(22), 2058, doi:10.1029/2002GL015438, 2002.

1. Introduction

[2] The Italian peninsula marks a convergent boundary between Africa and Europe where lithosphere underlying the Adriatic Sea dives beneath the lithosphere underlying the Tyrrhenian Sea [Dewey *et al.*, 1989]. This subduction process created the subaerial Italian peninsula via an uplift of the accretionary wedge. It is manifest presently in the distribution of deep earthquakes [Selvaggi and Amato, 1992] and in seismic tomography images [e.g., Lucente *et al.*, 1999; Wortel and Spakman, 2000]. Gravity field anomalies [Ballardin *et al.*, 1972] grow more negative from west to east across the peninsula, suggesting crustal thickening from the Tyrrhenian coast toward the Adriatic. Active-source seismology finds crustal thickness of ~ 25 km on the western side of the peninsula and ~ 35 km under the Apennines [de Franco *et al.*, 1998; Gualteri and Cassinis, 1998]. In the central part of the Italian peninsula the upper

25–30 km of the lithosphere are studied by active source seismic methods. The geometry of deployments degrades resolution near the coastline. P -tomography images reveal broader geometry of the convergent zone at depths in excess of 100 km (e.g., Lucente *et al.* [1999]). In this paper, we study P_S converted waves with teleseismic receiver functions (RFs) [Langston, 1977] to constrain the seismic structure in the upper ~ 100 km directly beneath a coastal seismic station. Previous studies of seismic anisotropy beneath the central part of the Italian peninsula identified an overall convergence-normal orientation of the fast propagation direction for both shear waves [Margheriti *et al.*, 1996] and P_n phases [Mele *et al.*, 1998]. At the Adriatic coast the pattern is less certain (Figure 1). The lack of depth resolution in shear-wave birefringence and the broad lateral averaging in P_n propagation complicate interpretations in terms of specific tectonic processes [Park and Levin, 2002]. P_S converted phases within the coda of teleseismic P waves offer unique constraints on the depth of anisotropic regions in the lithosphere and the upper mantle.

[3] During a 6-month period in 1994, an array of portable seismic observatories was deployed across the Northern Apennines [Margheriti *et al.*, 1996]. We analyzed seismic data from the easternmost node of that array, NAP9. Equipped with a LE-3D sensor, the station acquired sufficient data to explore directional and azimuthal variations in P_S converted phases. Useful data were concentrated within the NE quadrant (0 – 90° backazimuth). Other nearby nodes of the NAP array had much lower data recovery rates, precluding the extension of this study across the peninsula.

2. Receiver Functions

[4] We characterize P_S converted waves with a multitaper RF estimator [Park and Levin, 2000], and pay special attention to the direction- and distance-dependent behaviors of the observed wavefield (Figure 2).

[5] Through most of the observation range the radial RFs exhibit a large negative phase at 1.8 s. At 0 – 40° back-azimuth a coherent positive phase is seen also at 6 s. At 70° – 90° backazimuth a sequence of broad pulses arrives between 3 and 7 s, and possibly interferes with the 6-s pulse. The epicentral RF gather (Figure 2, right) shows that some P_S signals of this sequence arrive progressively later with increasing epicentral distance. This moveout is not consistent with upcoming converted waves in a 1-D structure. A two-sided (negative-positive) pulse is found between 8.5 and 10 s, most prominently in the 0 – 40° backazimuthal range. On the transverse RFs, the first motion displays a clear polarity reversal between backazimuthal ranges 0 – 40° (positive) and 60 – 90° (negative). A composite pulse appears at

¹Yale University, New Haven, Connecticut, USA.

²INGV, Rome, Italy.

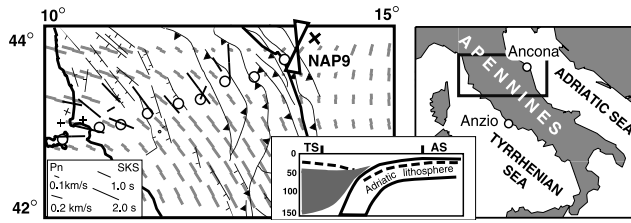


Figure 1. Geography, tectonics and seismic anisotropy indicators in the region. Solid lines show faults (normal - straight barbs, thrusts - triangular barbs). Circles - seismic stations of the Northern Apennines (NAP) profile. Seismic anisotropy indicators: shaded bars - fast P_n directions [Mele *et al.*, 1998], solid bars - fast polarization of birefringent SKS phases [Margheriti *et al.*, 2002] projected to the depth of 150 km. Observations of “null” shear-wave birefringence are shown by solid crosses. An “hour-glass” figure shows a range of acceptable orientations for the fast seismic velocity in the subcrustal mantle, inferred from RF analysis at station NAP9. The symbol is projected to 80 km depth. Margheriti *et al.* [1996] reported a number of birefringent shear phases with nearly north-south fast polarization at NAP9. Under more stringent selection criteria applied in a later paper only a “null” (no resolvable splitting) from backazimuth 52° was retained. A middle inset shows an overall geometry of subduction. Vertical bars: coastlines of the Tyrrhenian Sea (TS) and the Adriatic Sea (AS). Dashed lines: - crust-mantle transition; shaded outline - the asthenosphere, thought to invade due to slab rollback.

2–2.5 s at $0-60^\circ$ backazimuth, and is conspicuously absent in $60-90^\circ$ range. A sharp negative pulse at 5-s delay lies between backazimuths $10-40^\circ$, with less certain expression in the remainder of the observed range. A broad negative-positive phase is seen at 9–11 s, mainly between 40 and 90° . This phase weakens as source distance increases (see epicentral sweeps), and thus is likely to represent energy converted from an interface at depth.

[6] We seek a layered structure which predicts the behavior of those RF features that we judge to be consistent with a 1-D model. We develop models through trial-and-error, informed by observations of backazimuthal and epicentral P_S variation, the knowledge of the likely crust and upper-mantle rock properties, and the Occam’s Razor principle. The radial RFs are used to constrain a provisional velocity profile. The amplitude variation of the transverse component RFs diagnoses seismic anisotropy and/or the dip of model interfaces. We assume that anisotropy has hexagonal symmetry, with a “slow” axis in the crust and a “fast” axis in the mantle [Levin and Park, 1997]). The anisotropies of V_P and V_S are assumed to be equal. We compute reflectivity seismograms for upgoing compressional pulses at phase velocity 20 km/s and a range of backazimuths. This corresponds to an incidence angle $\sim 24^\circ$ within the subcrustal lithosphere, typical for P waves from sources $50-80^\circ$ away. We estimate RFs from these synthetics to compare with data-derived RFs, and modify the model until the waveforms are visually similar. We used starting mantle and crustal velocities typical for continental regions (mantle: $V_S = 4.6$ km/s; crust: $V_S = 3.65$ km/s) and V_P/V_S ratios of 1.78 and 1.75 for the crust and the mantle, respectively. We

interpret transverse signals with plausible moveout as resulting from anisotropy.

2.1. Preferred Model

[7] Figure 3 compares synthetic seismograms computed in the preferred model (Table 1) with averaged RFs for two distinct approach directions, 30° (northeastern) and 80° (eastern). A near-surface low velocity layer generates a large negative pulse at 1.8 s on the radial component, while anisotropy within that layer is responsible for the polarity inversion of the transverse RF first motion. The polarity change in the observed RFs (Figure 2) requires the symmetry axis within this shallow layer to be $\sim 50^\circ$ NE. A thin layer of anisotropy above a mild velocity increase at 17 km depth generates the transverse phase at 1.5 s. Aligning the symmetry axis towards 80° NE, with a 40° plunge from the horizontal, ensures that this phase is seen on the northeastern synthetic only. We interpret a positive phase at 6 s on the northeastern RF as the conversion from the crust-mantle interface at depth of 45 km. A strong velocity contrast in the model gives rise to well-developed multiples P_{ps} and P_{ss} which arrive at 20 and 25 s, respectively (not shown). Two broad pulses between 3 and 7 s on the eastern radial RF have a questionable P_S -delay behavior, and we chose not to model them. A transverse negative phase at 5 sec is matched by introducing an anisotropic layer with a symmetry axis pointing east, tilted up by 40° from the horizontal. Another anisotropic layer, with an axis plunging 30° from the horizontal towards 140° SE, yields a two-sided positive-negative transverse phase on the eastern synthetic between 4 and 5 s. A layer of decreased velocity in the upper mantle, between depths 78 and 89 km, generates plausible P_S pulses at 8–11 s on both radial and transverse RFs. Note that

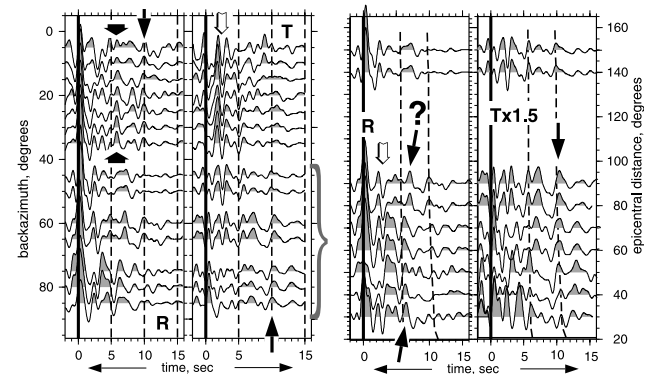


Figure 2. Receiver functions (RFs) for NAP9. RFs are computed in bins, with 50% overlap. Bin width is 10° for backazimuthal gathers, 20° for epicentral gathers. Spectral content limited at 0.75 Hz. Left panels show backazimuthal RF gathers, right panels show epicentral RF gathers in $40-90^\circ$ backazimuthal range (bracket on the backazimuthal sweep). Epicentral sweep of transverse RFs has amplitude boosted by 50% for visual clarity. Dashed lines show time marks in backazimuthal sweeps, predicted moveout curves for interfaces at 45 and 89 km in epicentral sweeps. Main interpreted phases: open arrow - midcrustal anisotropic layer; wide black arrow - Moho phase; vertical solid arrow - mantle phase. The slanted solid arrow shows a radial RF signal with moveout consistent with a surface-scattered wave.

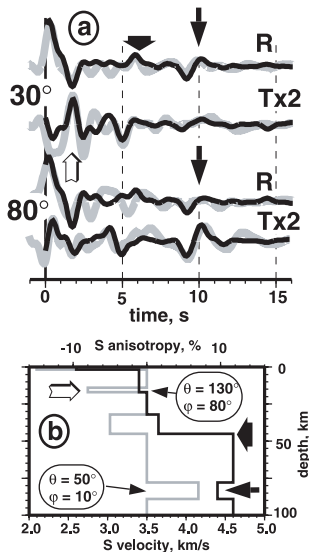


Figure 3. Comparison of observed RFs and synthetic seismograms computed for our preferred model (Table 1). (a) Observed average RFs (shaded) for two backazimuthal ranges: 0° – 30° (upper two traces), and 60° – 90° (lower two traces). Synthetic seismograms (solid) for backazimuths 30° and 80° . Features of the wavefield that we chose to model and corresponding elements of the velocity structure are marked with symbols as in Figure 2. (b) Velocity (solid) and anisotropy (shaded) beneath NAP9. Seismic anisotropy parameters (θ - tilt from vertical, ϕ - azimuth, clockwise from north) are annotated for the midcrustal anisotropic layer and the anisotropic layer in the mantle.

synthetic RFs correctly reproduce a lack of transverse energy on the northeastern RF and weak radial energy on the eastern RF. To achieve this, the fast symmetry axis of anisotropy in the layer points towards 10° NE, tilted up by 40° above the horizontal.

2.2. Uncertainties and Tradeoffs

[8] Strong transverse RF signals that vary predictably for earthquakes at different distances and backazimuths argue that a 1-D anisotropic model is appropriate for the crust beneath station NAP9. An alternative mechanism, namely, the dip of converging interfaces, seems unlikely in most cases. For instance, transverse phases associated with the crust-mantle transition (at ~ 5 s) could arise from a non-horizontal interface, but the implied dip of the interface would not align with the convergence direction. The sparse earthquake distribution in the dataset makes discrimination between dipping interfaces and anisotropy on the basis of P_S moveout with backazimuth [Levin and Park, 1997] difficult. Still, we note that the mid-crustal phase at 2–2.5 s (open arrow, Figure 2) maintains almost constant timing between backazimuths 0° and 60° . P_S phases (both radial and transverse) that define the upper-mantle phase at ~ 10 s (solid arrow, Figure 2) also maintain their timing over the backazimuthal range of observations. In both cases, coincident radial component signals are similar or smaller than the transverse component ones. In non-horizontal isotropic structures radial component should be larger than transverse [Cassidy, 1992]. However, an anisotropic interpretation for

the transverse RF polarity-switch at <1 -s delay time cannot be discriminated confidently from a very shallow strongly inclined feature. The assumption of “slow” and “fast” anisotropic symmetry in the crust and upper mantle, respectively, affects the outcome of the modeling. Choosing slow-axis anisotropy appears natural for the crust, where effect of layering, cracks and metapelite rocks likely dominate [Babuška and Cara, 1991]. In the subcrustal mantle, fast-axis anisotropy is commonly expected from deformed aggregates of olivine grains [Park and Levin, 2002]. Finally, the V_P/V_S ratio trades off with the depth of interfaces in the model. We experimented with V_P/V_S in the range 1.73–1.80, but interfaces within the crust and at its base do not deviate by more than 1–3 km from those reported in Table 1.

3. Discussion

[9] Significant features of the lithospheric structure implied by this study are (1) thick crust and (2) several depth intervals with pronounced rock fabric. Equally significant, however, is how few observed RF features associate simply with the Adriatic subduction geometry. From the orientation of principal stresses in the lithosphere [Montone et al., 1999] one may expect fabrics with NE–SW lineations (along the convergence direction) or NW–SE lineations (along the Apennines mountain belt and normal to the principal stress direction), as well as inclined fabric dipping to the SW. All of these geometries should lead to polarity switches in the transverse RF within the NE backazimuthal quadrant densely sampled by our dataset. Surprisingly, only the first motion of the transverse RF, sensitive to near-surface structure, exhibits a polarity switch at $\sim 50^\circ$ backazimuth.

3.1. Midcrustal Anisotropic Zone

[10] Our model suggests a zone of rock texture at depth of ~ 15 km, with the axis plunging eastward. A midcrustal decollement between the Adriatic lithosphere and the overriding Apenninic crustal wedge is known from seismic reflection data (e.g., Guidici and Gualteri [1998]). Inclined rock fabric developed via simple shear within a decollement zone could explain the anisotropic layer we propose in our model. The symmetry axis plunges towards 80° NE, implying that the local shear direction within the decollement deviates from the more northerly direction expected from

Table 1. Anisotropic Velocity Model Consistent With Receiver Functions at NAP9

z (km)	$V_P, \frac{\text{km}}{\text{s}}$	$V_S, \frac{\text{km}}{\text{s}}$	$\rho, \frac{\text{g}}{\text{cm}^3}$	$B, \%$	$E, \%$	θ, deg	ϕ, deg
1.8	4.5	2.6	2.3	–15	–15	130	50
14	6	3.4	2.6
17	6	3.4	2.6	–8	–8	130	80
32	6.125	3.5	2.8
38	6.4	3.65	2.8	–5	–5	120	140
45	6.4	3.65	2.8	–5	–5	50	90
78	8.2	4.6	3.3
89	7.8	4.4	3.1	7	7	50	10
∞	8.2	4.6	3.3

Depth z indicates the bottom of each layer. The parameters B and E scale peak-to-peak variations of compressional and shear velocity, respectively, each with $\cos 2\eta$ azimuthal dependence [Levin and Park, 1997]. The angles θ and ϕ define the tilt (from vertical) and strike (clockwise from north) of the axis of symmetry within each anisotropic layer.

the overall Apennine thrust system geometry. However, many individual thrusts turn southward around Ancona (Figure 1), suggesting local reorientation of the stress field at depth.

3.2. Crust-Mantle Transition

[11] We interpret the radial P_S signal at ~ 6 s seen in northeastern composite RF (Figure 3) as a conversion at the crust-mantle interface, implying crustal thickness ~ 45 km. This phase is one-sided and quite tight, suggesting a sharp transition in properties. We ignore an arrival in this time frame on the eastern composite RF, because it exhibits reverse moveout (Figure 2). Our crustal thickness value diverges from that of ~ 35 km, commonly found in the literature (e.g., Morelli [1998]). To our knowledge, estimates of the crustal thickness beneath the Adriatic coast are extrapolated from areas further inland. Using refraction data from the CROP3 transect *De Franco et al.* [1998] estimate crustal thickness there at ~ 35 km. However, raypath coverage of this cross-peninsula refraction survey is not optimal for evaluating properties beneath the coast. Notably, north of Ancona *Gualteri and Cassinis* [1998] fail to identify specific reflections from the Moho beneath the coastline, but report numerous reflective features at depths in excess of 40 km. This later observation is consistent with complicated anisotropy we find in the lowermost crustal (32–45 km depth) part of our model, and a crust-mantle transition at 45 km. Due to spectral content, teleseismic waves may detect as “sharp” a feature that appears diffuse in reflection data. Furthermore, since in our RFs the 6s conversion is restricted to the 0° – 40° range of backazimuths, we can only infer it as a “local” feature. The area near Ancona is enclosed within a local gravity high superimposed over a broad negative trend [*Ballardin et al.*, 1972], making it likely that structure here differs from elsewhere along the Adriatic coast.

3.3. Anisotropic Layer in the Mantle

[12] The orientation of fast wavespeed within the 78–89 km deep anisotropic layer is $10^\circ\text{NE} \pm 10^\circ$. This direction is similar to Pn anisotropy [*Mele et al.*, 1998] direction and to some SKS splitting results found at NAP9 and in the surrounding area [*Margheriti et al.*, 2002] (Figure 1). However, this layer is too deep to be seen by Pn, and relatively thin to influence splitting of a long-period teleseismic shear wave. Also, shear-wave splitting observations are too sparse to provide a discriminant between vertical and lateral variations in anisotropic properties in the region.

[13] The depth range of the mantle anisotropic layer in our model places it either within the Adriatic lithosphere, or directly beneath it. In the first case, the frozen rock fabric may be inherited from tectonic events that shaped Adriatic lithosphere. The fabric could be formed by the deformation along the “Ancona-Anzio line”, a presently inactive lithospheric-scale transcurrent zone [*Calamita and Deiana*, 1988]. This transcurrent feature would have to be common to both the upper and the lower plates of the convergent margin. The alternative interpretation, of dynamically maintained fabric beneath the lithosphere, is appealing because active rollback of the Adriatic slab should drive sublitho-

spheric mantle flow beneath it. We speculate that irregularities in the slab [e.g., *Lucente et al.*, 1999] modulate that flow considerably, yielding the local deformation regime suggested by the mantle anisotropy indicators in RFs observed on the Adriatic coast of Italy.

[14] **Acknowledgments.** This research was supported by the NSF grant EAR-0106867 (VL and JP). We used GMT software [*Wessel and Smith*, 1991] to prepare figures. Steven Roecker and an anonymous reviewer made helpful suggestions.

References

- Babuška, V., and M. Cara, *Seismic Anisotropy in the Earth*, Kluwer Academic, Dordrecht, 1991.
- Ballardin, S., B. Palla, C. Trombetti, The construction of the gravimetric map of Italy, Pub. d Commiss. Geod. It., 3rd series, Memour 19, Firenze, 991, 1972.
- Calamita, F., and G. Deiana, The arcuate shape of the Umbria-marche-Sabina Apennines (Central Italy), *Tectonophysics*, 146, 139–147, 1988.
- Cassidy, J. F., Numerical experiments in broadband receiver function analysis, *Bull. Seismol. Soc. Am.*, 82, 1453–1474, 1992.
- Dewey, J. K., M. L. Helman, D. H. W. Hutton, and S. D. Knot, Kinematics of the western Mediterranean, *Geol. Soc. Sp. Pub.*, 45, 265–283, 1989.
- De Franco, R., F. Ponziani, G. Biella, G. Boniolo, G. Caielli, A. Corsi, M. Maistrello, and A. Morrone, DSS-WAR experiment in support of the CROP03 project, *Mem. Geo. Soc. It.*, 52, 67–90, 1998.
- Gualteri, L., and R. Cassinis, The deep structure of the Northern Apennines imaged by ray tracing depth migration of near-vertical seismic data, *Mem. Geo. Soc. It.*, 52, 163–174, 1998.
- Guidici, M., and L. Gualteri, Application of revised ray tracing migration to imagine lateral variations of seismic fabric corresponding to different tectonic styles in the northern Apennines, *Tectonoph.*, 300, 181–197, 1998.
- Langston, C. A., Corvallis, Oregon, crustal and upper mantle receiver structure from teleseismic P and S waves, *Bull. Seismol. Soc. Am.*, 67, 713–724, 1977.
- Levin, V., and J. Park, P-SH conversions in a flat-layered medium with anisotropy of arbitrary orientation, *Geophys. J. Int.*, 131, 253–266, 1997.
- Lucente, F., C. Chiarabba, and G. Cimini, Tomographic constraints on the geodynamic evolution of the Italian region, *J. Geophys. Res.*, 104(B9), 20,307–20,327, 1999.
- Margheriti, L., C. Nostro, M. Cocco, and A. Amato, Seismic anisotropy beneath the Northern Apennines (Italy) and its tectonic implications, *Geophys. Res. Lett.*, 23(20), 2721–2724, 1996.
- Margheriti, L., F. P. Lucente, and S. Pondrelli, SKS Splitting measurements in the Apenninic-Tyrrhenian domain (Italy) and their relation with Lithospheric subduction and mantle convection, *J. Geophys. Res.*, in press, 2002.
- Mele, G., A. Rovelli, D. Seber, T. M. Hearn, and M. Barazangi, Compression velocity structure and anisotropy in the uppermost mantle beneath Italy and surrounding regions, *J. Geophys. Res.*, 103, 12,529–12,543, 1998.
- Montone, P., A. Amato, and S. Pondrelli, Active Stress Map of Italy, *J. Geophys. Res.*, 104, 25,595–25,610, 1999.
- Morelli, C., Lithospheric structure and geodynamics of the Italian Peninsula derived from geophysical data: a review, *Mem. Geo. Soc. It.*, 52, 113–122, 1998.
- Park, J., and V. Levin, Receiver functions from multiple-taper spectral correlation estimates, *Bull. Seismol. Soc. Am.*, 90, 1507–1520, 2000.
- Park, J., and V. Levin, Seismic Anisotropy, Subsurface Rock Textures, and Upper-Mantle Geodynamics, *Science*, 296, 485–489, 2002.
- Selvaggi, G., and A. Amato, Subcrustal earthquakes in the Northern Apennines (Italy): Evidence for a still active subduction?, *Geophys. Res. Lett.*, 19(21), 2127–2130, 1992.
- Wessel, P., and W. H. F. Smith, Free software helps map and display data, *EOS*, 72, 441, 445–446, 1991.
- Wortel, M., and W. Spakman, Subduction and slab detachment in the Mediterranean-Carpathian region, *Science*, 290, 1910–1917, 2000.